ISSN 1674-1056
http://cpb.iphy.ac.cn
http://iopscience.iop.org/cpb
中国物理 B
Chinese Physics
中国物理 Chinese Physics B

Fe: ZnSe laser pumped by a 2.93-μm Cr, Er: YAG laser

Ying-Yi Li(李英一), Tong-Yu Dai(戴通宇), Xiao-Ming Duan(段小明), Chun-Fa Guo(郭春发), Li-Wei Xu(徐丽伟), You-Lun Ju(鞠有伦)

Citation: Chin. Phys. B . 2019, 28(6): 064203. **doi:** 10.1088/1674-1056/28/6/064203
Journal homepage: http://cpb.iphy.ac.cn; http://iopscience.iop.org/cpb

What follows is a list of articles you may be interested in

Optically manipulated nanomechanics of semiconductor nanowires

Chenzhi Song(宋晨之), Shize Yang(杨是赜), Xiaomin Li(李晓敏), Xiao Li(李晓), Ji Feng(冯济), Anlian Pan(潘安练), Wenlong Wang(王文龙), Zhi Xu(许智), Xuedong Bai(白雪冬)
Chin. Phys. B . 2019, 28(5): 054204. **doi:** 10.1088/1674-1056/28/5/054204

Anisotropic stimulated emission cross-section measurement in Nd: YVO_4

Rui Guo(郭瑞), Yijie Shen(申艺杰), Yuan Meng(孟鸢), Mali Gong(巩马理)
Chin. Phys. B . 2019, 28(4): 044204. **doi:** 10.1088/1674-1056/28/4/044204

Propagation of a Pearcey beam in uniaxial crystals

Chuangjie Xu(许创杰), Ludong Lin(林露东), Zhengzhong Huang(黄郑重), Donglong He(何东龙), Dongmei Deng(邓冬梅)
Chin. Phys. B . 2019, 28(2): 024201. **doi:** 10.1088/1674-1056/28/2/024201

Effect of Hf^{4+} doping on structure and enhancement of upconversion luminescence in Yb: Tm: $LiNbO_3$crystals

Li Dai(代丽), Chunrui Liu(刘春蕊), Xianbo Han(韩县博), Luping Wang(王路平), Yu Shao(邵瑀), Yuheng Xu(徐玉恒)
Chin. Phys. B . 2018, 27(11): 114217. **doi:** 10.1088/1674-1056/27/11/114217

Energy scaling and extended tunability of a ring cavity terahertz parametric oscillator based on $KTiOPO_4$crystal

Yuye Wang(王与烨), Yuchen Ren(任宇琛), Degang Xu(徐德刚), Longhuang Tang(唐隆煌), Yixin He(贺奕焮), Ci Song(宋词), Linyu Chen(陈霖宇), Changzhao Li(李长昭), Chao Yan(闫超), Jianquan Yao(姚建铨)
Chin. Phys. B . 2018, 27(11): 114213. **doi:** 10.1088/1674-1056/27/11/114213

Fe:ZnSe laser pumped by a 2.93-μm Cr, Er:YAG laser*

Ying-Yi Li(李英一), Tong-Yu Dai(戴通宇), Xiao-Ming Duan(段小明), Chun-Fa Guo(郭春发), Li-Wei Xu(徐丽伟), and You-Lun Ju(鞠有伦)†

National Key Laboratory of Tunable Laser Technology, Harbin Institute of Technology, Harbin 150001, *China*

(Received 19 February 2019; revised manuscript received 19 April 2019; published online 29 May 2019)

We demonstrated an Fe:ZnSe laser pumped by a 2.93-μm Cr, Er:YAG laser at liquid nitrogen and room temperature in single-shot free-running operation for the first time. The xenon flash lamp pumped Cr, Er:YAG laser had a maximum single pulse energy of 1.414 J, and the threshold and slope efficiency were 141.70 J and 0.70% which were respectively reduced by 29.3% and increased by 52.2% compared with the Er:YAG laser. At liquid nitrogen temperature of 77 K, the maximum single pulse energy of the Fe:ZnSe laser was 197.6 mJ, corresponding to a slope efficiency of 13.4%. The central wavelength and full width at half maximum (FWHM) linewidth were 4037.4 nm and 122.0 nm, respectively. At room temperature, the laser generated a maximum single pulse energy of 3.5 mJ at the central wavelength of 4509.6 nm with an FWHM linewidth of 171.5 nm.

Keywords: Fe:ZnSe, Cr, Er:YAG, Er:YAG, free-running

PACS: 42.55.Rz, 42.60.Da, 42.60.Jf **DOI:** 10.1088/1674-1056/28/6/064203

1. Introduction

The 3 μm–5 μm lasers have played an import role in many fields, such as scientific research, industrial production and medical care.[1,2] In the last two decades, as a medium could generate lasers over this spectral range directly, the Fe:ZnSe crystal has attracted much attention. The first Fe:ZnSe laser pumped by a 2.698-μm Er:YAG laser was reported by Adams in 1999.[3] From then on, the Er:YAG, Er:YSGG, Cr:ZnSe, HF, and other lasers which had the wavelength around 3 μm were employed as the pump.[4] Up to now, the HF lasers and xenon flash lamp pumped Er:YAG lasers have been the primary pumps for the high energy Fe:ZnSe lasers while the other pumps generated the Fe:ZnSe lasers with the output energy of several millijoules or less.[4] The HF lasers are usually employed as the pumps for short-pulse-duration Fe:ZnSe lasers at room temperature,[5–12] and the Fe:ZnSe lasers and the pump both have the pulse durations of 100 ns–200 ns. For high energy Fe:ZnSe lasers with long pulse duration, the free-running 2.94-μm Er:YAG lasers at low temperature are the efficient pumps which have the pulse durations of several hundreds of microseconds.[13,14]

Although Er:YAG is widely used as the gain medium to generate the 2.94-μm lasers, the self-terminal state, in which the lifetime of the upper level $^4I_{11/2}$ (0.1 ms) is far less than that of the lower $^4I_{13/2}$ (6 ms), goes against the population inversion.[15] Doping the sensitizer Cr^{3+} into the Er:YAG is benefit to the laser operation because Cr^{3+} has two broad absorption bands in the red and blue–green wavelength regions corresponding to the transitions from $^4A_2$ to $^4T_2$ and $^4T_1$ energy levels, which overlap well with the emission of the xenon flash lamp.[16] The transfer of the excitation from Cr^{3+} to the $^4F_{9/2}$ level and the cross-relaxation together populate the $^4I_{11/2}$ level, which weakens the self-terminal state,[17,18] as shown in Fig. 1.

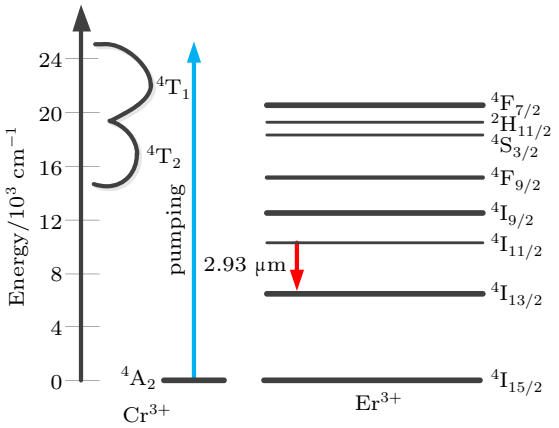


Fig. 1. Energy diagram of Cr^{3+} and Er^{3+}.

In this work, we demonstrated an Fe:ZnSe laser pumped by a Cr, Er:YAG laser in single-shot free-running mode for the first time. For the xenon flash lamp pumped Cr, Er:YAG laser, a maximum single pulse energy of 1.414 J was obtained. The threshold was reduced by 29.3% and the slop efficiency was increased by 52.2%, compared with the Er:YAG laser under the same condition. For the Fe:ZnSe laser, at liquid nitrogen and room temperature, the maximum output energies were 197.6 mJ and 3.5 mJ, the central wavelengths were 4037.4 nm and 4509.6 nm, corresponding to the slop efficiency of 13.4% and 0.27%, respectively.

*Project supported by the National Natural Science Foundation of China (Grant No. 61405047).

†Corresponding author. E-mail: juyoulun@126.com

© 2019 Chinese Physical Society and IOP Publishing Ltd

2. Xenon flash lamp pumped Cr, Er:YAG, and Er:YAG lasers

The optical schematic diagram of the Cr, Er:YAG, and Er:YAG lasers is shown in Fig. 2. The Cr, Er:YAG crystal doped with 0.8 at.% Cr^{3+} and 50-at.% Er^{3+}, the Er:YAG crystal doped with 50-at.% Er^{3+} both had a diameter of 5 mm and a length of 150 mm. The circular facets of the two crystals were anti-reflection coated at 2700 nm–3100 nm. Two xenon flash lamps with the electric arc of 140 mm were placed into the double-ellipse condenser cavity. The minimum pulse width of the lamps was 200 μs with the maximum voltage of 2000 V in our power supply system which ran in single-shot mode. The crystals and lamps were cooled in the deionized water at a temperature of 20 °C. The 324-mm-long straight cavity was composed of a flat rear mirror M1 (high-reflection coated at 2700 nm–3100 nm) and an output coupler M2 (curvature radius equals −1500 mm, and transmittance equals 28.5% at 2700 nm–3100 nm).

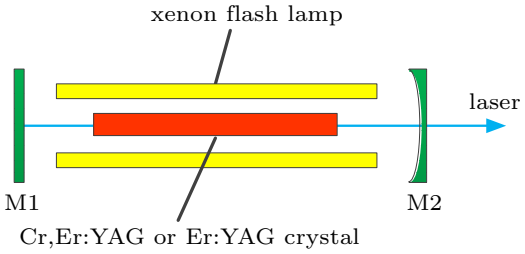


Fig. 2. Schematic diagram of the Cr, Er:YAG/Er:YAG laser.

Figure 3 shows the output pulse energy versus the incident pump energy for the Er:YAG and Cr, Er:YAG lasers. The output pulse energy was measured with the Joule meter Coherent J-50MB-YAG-IR (energy range: 1 mJ–3 J) and the energy of the flash lamp was calculated with the formula $E = 0.5CU^2$, where C and U presents the capacitance and voltage of the capacitor, respectively.

For the Er:YAG laser, the maximum pulse energy was 0.941 J with the pump energy of 400 J. The calculated threshold and slope efficiency were 200.45 J and 0.46%, respectively. While for the Cr, Er:YAG laser, the maximum pulse energy was 1.414 J with the pump energy of 342.25 J. We did not inject the whole pump energy of 400 J to avoid the coating films of the crystal or mirrors being damaged. The calculated threshold and slope efficiency were 141.70 J and 0.70%, which were respectively reduced by 29.3% and increased by 52.2% compared with the Er:YAG laser.

The temporal characteristics of the Cr, Er:YAG laser and flash lamp were detected simultaneously by a PbSe detector (spectral range: 1000 nm–4700 nm, response time: 1 μs) and a silicon pin photodiode (spectral range: 200 nm–1100 nm, response time: 50 ns) respectively, and recorded by a Tektronix MSO 3034 digital oscilloscope (sampling rate: 2.5 GS/s, bandwidth: 300 MHz). A typical temporal profile is shown in Fig. 4, and the pulse duration of the Cr, Er:YAG laser was about 200 μs.

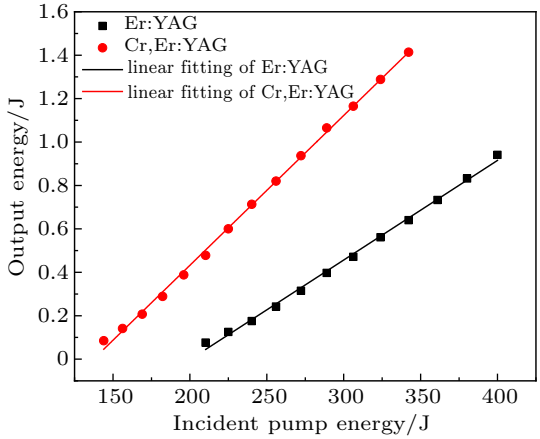


Fig. 3. Output pulse energy versus incident energy of the Cr, Er:YAG/Er:YAG laser.

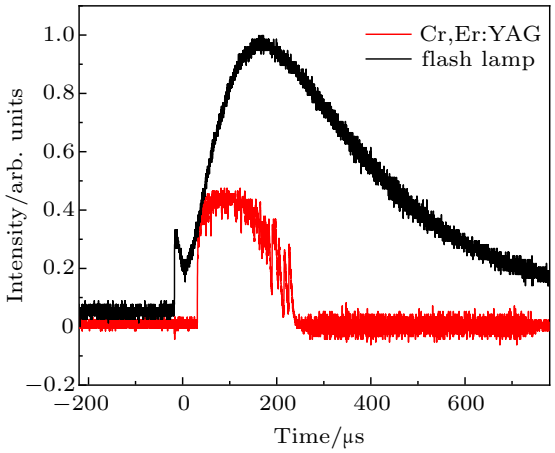


Fig. 4. Temporal profile of the Cr, Er:YAG laser (red) and flash lamp (black).

The wavelength of the Cr, Er:YAG laser was recorded with the help of a WDG-30 monochromator (resolution: 0.3 nm). At the maximum pulse energy of 1.414 J, the wavelength covered the range of 2923 nm–2940 nm, centered at 2931.2 nm with a full width at half maximum (FWHM) of 10 nm according to the Gauss fitting, as shown in Fig. 5.

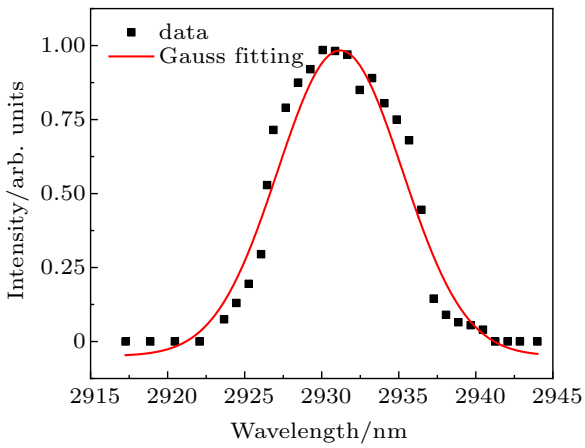


Fig. 5. Output spectrum of the Cr, Er:YAG laser.

3. Fe:ZnSe laser pumped by the Cr, Er:YAG laser

As described above, we obtained a Cr, Er:YAG laser in single-shot free-running mode. As the central wavelength of the Cr, Er:YAG laser was near the absorption peak of the Fe:ZnSe crystal,[19] we took advantage of this laser as a pump for the Fe:ZnSe laser.

The optical schematic diagram of the Fe:ZnSe laser is shown in Fig. 6.

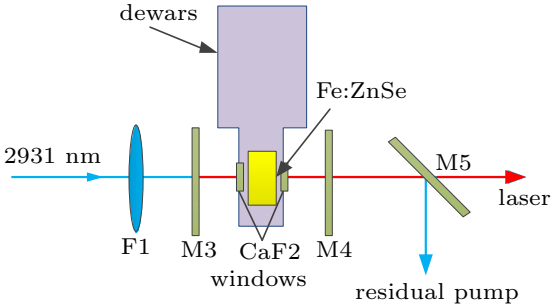


Fig. 6. Schematic diagram of the Fe:ZnSe laser.

The 50-mm-long straight cavity was composed of a flat input mirror M3 (high-transmission coated at 2700 nm–3100 nm and high-reflection coated at 3800 nm–4700 nm) and an output coupler M4 (coated with different transmittances at 3800 nm–4700 nm). A 45° dichroic mirror M5 was placed behind M4 to filtrate the residual pump.

The Fe:ZnSe crystal, the dimension of which was 4 mm in thickness and 10 mm × 10 mm in cross-section, was grown by high-pressure vertical zone melting with the Fe^{2+} doping concentration of $5 \times 10^{18}/cm^3$. The two working facets were uncoated, high-quality polished, and parallel to each other within 30″. The crystal was wrapped by indium foil and mounted in a copper heat sink. The crystal temperature was controlled by a liquid nitrogen cooled cryogenic vacuum Dewars, which had two parallel plane uncoated CaF_2 windows aligned perpendicular to the optical axis of the cavity, and detected by a thermocouple of PT100. The Cr, Er:YAG laser was focused via F1 and injected into the center of the Fe:ZnSe crystal along the optical axis.

We have a study on the Fe:ZnSe laser at liquid nitrogen temperature of 77 K and room temperature of 298 K. The measuring instruments were the same as that used in the Cr, Er:YAG laser.

Figure 7 shows the output pulse energy versus incident energy of the Fe:ZnSe laser at 77 K. The maximum pulse energy of 197.6 mJ was obtained under the incident pump energy of 1.38 J when the flat output coupler with a transmittance equal to 50% was used, corresponding to a slope efficiency of 13.4%.

Figure 8 shows a typical temporal profile of the Fe:ZnSe laser at 77 K, which has the similar shape with the Cr, Er:YAG laser.

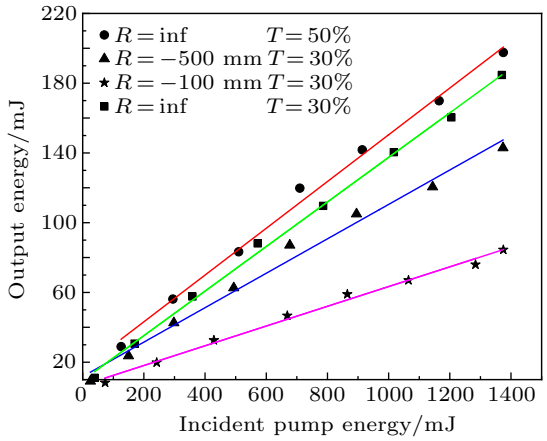


Fig. 7. Output pulse energy *versus* incident energy of the Fe:ZnSe laser at 77 K (R and T represent the curvature radius and transmittance of M4, respectively).

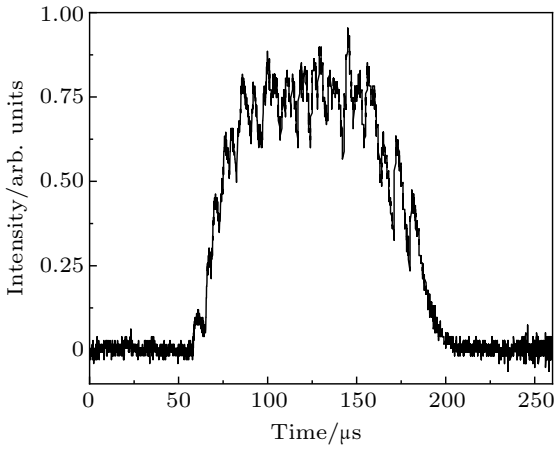


Fig. 8. Temporal profile of the Fe:ZnSe laser at 77 K.

The central wavelength of the Fe:ZnSe laser at 77 K was 4037.4 nm with an FWHM linewidth of 122.0 nm according to the Gauss fitting, which is shown in Fig. 9.

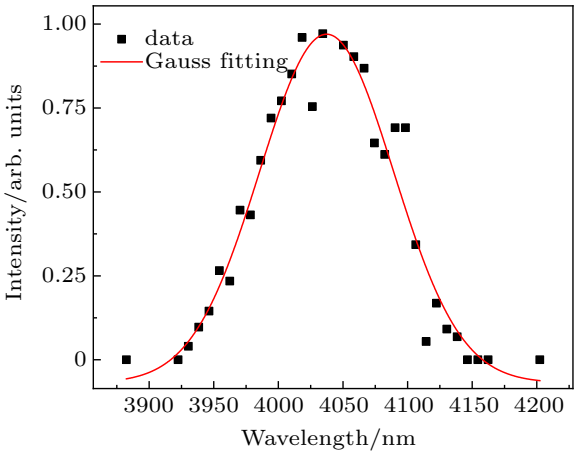


Fig. 9. Output spectrum of the Fe:ZnSe laser at 77 K.

Figure 10 shows the output pulse energy versus incident energy of the Fe:ZnSe laser at 298 K. Although the lifetime of upper energy level was as short as 370 ns at room temperature, we still acquired the lasing output on account of the spiked nature of the pump.[13] The maximum pulse energy of 3.5 mJ

was obtained under the incident pump energy of 1.38 J when the flat output coupler with a transmittance equal to 30% was used, corresponding to a slope efficiency of 0.27%.

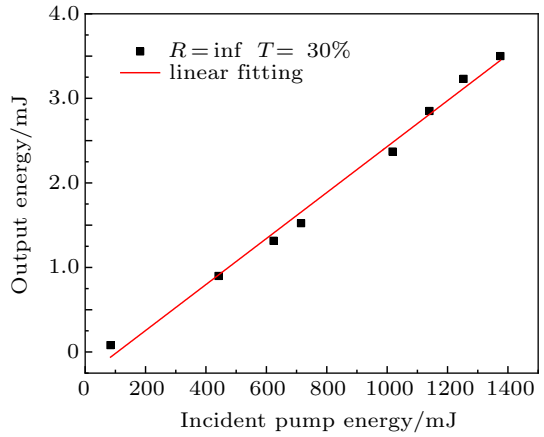


Fig. 10. Output pulse energy versus incident energy of the Fe:ZnSe laser at 298 K.

Figure 11 shows a temporal profile of the Fe:ZnSe laser at 298 K, the pulse duration of which was sharper and shorter compared with that at 77 K.

The central wavelength of the Fe:ZnSe laser at 298 K was 4509.6 nm with an FWHM linewidth of 171.5 nm according to the Gauss fitting, which is shown in Fig. 12. It had a redshift of about 470 nm compared with that at 77 K.

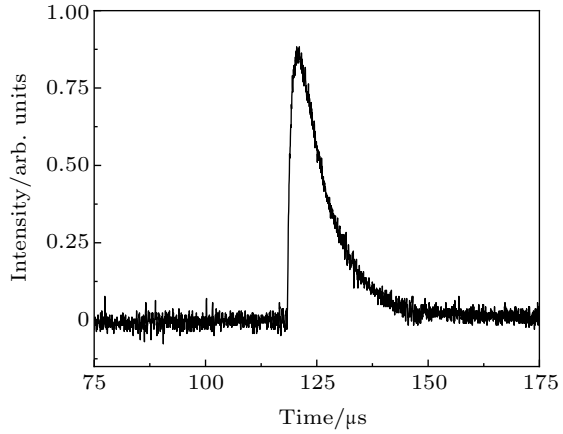


Fig. 11. Temporal profile of the Fe:ZnSe laser at 298 K.

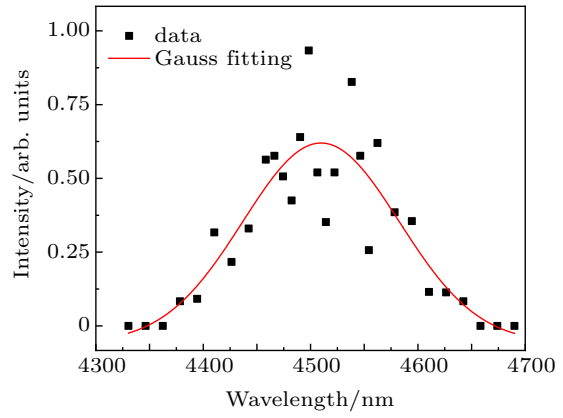


Fig. 12. Output spectrum of the Fe:ZnSe laser at 298 K.

4. Conclusion

In conclusion, we demonstrated an Fe:ZnSe laser in single-shot free-running operation pumped by a Cr, Er:YAG laser for the first time. The maximum single pulse energy of the Cr, Er:YAG laser was 1.414 J, the threshold and slope efficiency were reduced by 29.3% and increased by 52.2% compared with the Er:YAG laser due to the doping iron of Cr^{3+}, which weakened the self-terminal state. The maximum single pulse energy and central wavelength of the Fe:ZnSe laser were 197.6 mJ and 4037.4 nm at 77 K, respectively, in contrast to 3.5 mJ and 4509.6 nm at room temperature. A higher single pulse energy could be obtained by increasing the pump energy because the gain was not saturated. This work demonstrated that Cr, Er:YAG is a more effective crystal to generate the 2.93-μm laser compared with Er:YAG, and the Cr, Er:YAG laser is a feasible pump for the Fe:ZnSe crystal to generate the 3 μm–5 μm lasers.

References

[1] Chang J H, Sun Q, Ge Y X, Wang T T, Tao Z H and Zhang C 2013 *Chin. Phys. B* **22** 124204
[2] Li G, Zhou Y, Li S J, Yao P J, Gao W Q, Gu C and Xu L X 2018 *Chin. Phys. Lett.* **35** 114203
[3] Adams J J, Bibeau C, Page R H, Krol D M, Furu L H and Payne S A 1999 *Opt. Lett.* **24** 1720
[4] Mirov S B, Fedorov V V, Martyshkin D, Moskalev I S, Mirov M and Vasilyev S 2015 *IEEE J. Sel. Top. Quantum Electron.* **21** 1601719
[5] Gavrishchuk E M, Kazantsev S Y, Kononov I G, Rodin S A and Firsov K N 2014 *Quantum Electron.* **44** 505
[6] Firsov K N, Gavrishchuk E M, Kazantsev S Y, Kononov I G and Rodin S A 2014 *Laser Phys. Lett.* **11** 085001
[7] Velikanov S D, Zaretskiy N A, Zotov E A, Kozlovsky V I, Korostelin Y V, Krokhin O N, Maneshkin A A, Podmar'kov Y P, Savinova S A, Skasyrsky Y K, Frolov M P, Chuvatkin R S and Yutkin I M 2015 *Quantum Electron.* **45** 1
[8] Firsov K N, Frolov M P, Gavrishchuk E M, Kazantsev S Y, Kononov I G, Korostelin Y V, Maneshkin A A, Velikanov S D, Yutkin I M, Zaretsky N A and Zotov E A 2016 *Laser Phys. Lett.* **13** 015002
[9] Dormidonov A E, Firsov K N, Gavrishchuk E M, Ikonnikov V B, Kazantsev S Y, Kononov I G, Kotereva T V, Savin D V and Timofeeva N A 2016 *Appl. Phys. B* **122** 211
[10] Velikanov S D, Zaretsky N A, Zotov E A, Kazantsev S Y, Kononov I G, Korostelin Y V, Maneshkin A A, Firsov K N, Frolov M P and Yutkin I M 2016 *Quantum Electron.* **46** 11
[11] Pan Q K, Xie J J, Chen F, Zhang K, Xiao F, Yu D Y, He Y, Sun J J, Zhang L M and Guo J 2018 *Chin. J. Lasers* **45** 1101101 (in Chinese)
[12] Kong X Y, Ke C J, Wu T H and Hang Y 2018 *Infrared Laser Eng.* **47** 1005001 (in Chinese)
[13] Frolov M P, Korostelin Y V, Kozlovsky V I, Mislavskii V V, Podmar'kov Y P, Savinova S A and Skasyrsky Y K 2013 *Laser Phys. Lett.* **10** 125001
[14] Frolov M P, Korostelin Y V, Kozlovsky V I, Podmar'kov Y P and Skasyrsky Y K 2018 *Opt. Lett.* **43** 623
[15] Ziolek C, Ernst H, Will G F, Lubatschowski H and Welling H 2001 *Opt. Lett.* **26** 599
[16] Moulton P F, Manni J G and Rines G A 1988 *IEEE J. Quantum Electron.* **24** 960
[17] Gross R, Huber G, Struve B and Duczinski E 1991 *J. Phys. IV* **1** 363
[18] Voron'ko Y K, Gessen S B, Gribkov I V, Osiko V V, Ryabochkina P A, Tatarintsev V M, Ushakov S N and Tsymbal L I 1990 *Sov. J. Quantum Electron.* **20** 923
[19] Demirbas U, Sennaroglu A and Somer M 2006 *Opt. Mater.* **28** 231